ACS APPLIED MATERIALS & INTERFACES

Research Article

Cite This: ACS Appl. Mater. Interfaces 2018, 10, 11776−11784

www.acsami.org

Low-Power All-Organic Electrophoretic Display Using Self-Assembled Charged Poly(*t*-butyl methacrylate) Microspheres in Isoparaffinic Fluid

Kyeong Hyeon Ko,[†,§] Eunseon Park,[†,§] Hyunjung Lee,[‡] and Wonmok Lee*[,†]

[†]Department of Chemistry, Sejong University, 98 Gunja-dong, Gwangjin-gu, Seoul 143-747, Korea

[‡]School of Advanced Materials Engineering, Kookmin University, 861-1 Jeongneung-dong, Seoul 136-702, Korea

Supporting Information

ABSTRACT: The increasing demands for display devices with low power consumption and outdoor readability have stimulated comprehensive research into full-color reflective displays that employ color-tunable photonic crystal technologies. Although the recently developed crystalline colloidal arrays (CCAs) of the charged microspheres have shown the outstanding color tunability, the practical application is limited because the use of highly polar liquid medium such as water is required to maintain the charges on the surface of microsphere, whereas it is not suitable for long-term use in an electric field. Herein, a self-assembled CCA from charged poly(*t*-butyl methacrylate) microspheres was successfully fabricated, which was stabilized by the charged inverse micelles of sodium di-2-ethylhexyl-sulfosuccinate in a nonpolar isoparaffinic fluid. A charged all-organic CCA was found to exhibit full-color tunability with a 1000-fold reduction in the power consumption (~6 μW cm^{-2}) under a direct current voltage bias of 4 V in comparison to that in an aqueous system, which is a promising feature for a low-power-consumption display device.

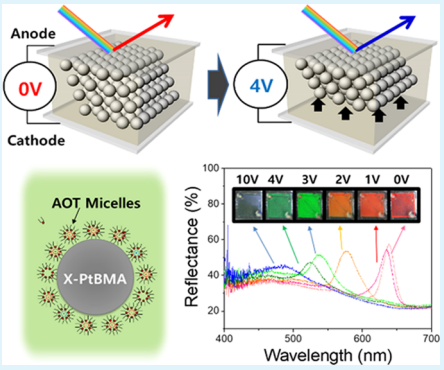

KEYWORDS: *reflective display, electrophoretic display, crystalline colloidal array, cross-linked poly(t-butyl methacrylate), all organic, low power*

1. INTRODUCTION

Undoubtedly, color display devices possess a huge market share in visual communication technologies, such as TVs, computer monitors, mobile phones, etc. Currently, flat-panel liquid crystal displays and light-emitting diodes are the two principal technologies in the display industry. However, their high power consumption remains the most problematic issue for both devices, particularly mobile applications.[1,2] For instance, approximately 80% of the battery power of a mobile phone is consumed by the display modules. Reflective displays are regarded as an alternative display technology, which utilize room light or sunlight to generate a color contrast, thereby eliminating the need of electric power for lighting. From the viewpoint of power consumption and considering other advantageous features, paperlike reflective displays are good candidates for applications requiring low power consumption, such as wallpapers, billboards, and bus station displays. Therefore, these displays have recently received considerable attention in the field of visual communication. A representative example of a reflective display device is the electrophoretic display (e.g., E ink), which involves the liquid dispersion of negatively charged white inorganic particles and positively charged black particles placed between two parallel conductive plates.[3] When a positive voltage is applied to the transparent top plate, electrophoretic migration of the white particles occurs and white color appears due to the reflection of light. The application of an opposite voltage bias will generate black color due to the migration of black particles toward the top plate. The fabrication of two-dimensional pixel arrays using electrophoretic displays coupled with microcapsule technology gave birth to electronic paper.[4] However, E ink can only generate black and white contrast. To produce a full-color E ink display, red, green, and blue (RGB) color filters should be placed on top of each pixel, where the loss of light is inevitable. Together with E ink technology, Bragg's diffraction of room light from the electrically tunable photonic crystal (PC) structure was utilized to obtain a full-color reflective display with minimum loss of light.[5,6] For instance, multilayers especially composed of block-copolymers are promising due to the easy fabrication.[7] However, the system needs a higher electric field (E-field) to fully manipulate photonic color from blue to red and the response time is rather slow. Among successful developments of self-assembled colloidal PC structures for reflective display, a crystalline colloidal array (CCA) of microspheres (μ-spheres) has been extensively employed due to its simplicity and versatility for fabrication.[6] In

Received: November 10, 2017
Accepted: March 23, 2018
Published: March 23, 2018

DOI: 10.1021/acsami.7b17122
ACS Appl. Mater. Interfaces 2018, 10, 11776−11784

Table 1, recent developments of colloid-based display devices over the last decade are summarized.

Table 1. Recent Developments of Electrically Tunable Three-Dimensional Photonic Crystal based on Colloidal Arrays

microspheres	dispersing medium	advantages	possible disadvantage	ref
SiO_2	PFS[a]	bistability and color tunability	difficult synthesis	8
TiO_2	ethylene glycol	high index and stability	poor color tunability	17
SiO_2@Fe_2O_3	propylene carbonate	low angular dependence	difficult synthesis	14
TiO_2@SiO_2	propylene carbonate	high index contrast and stability	color tunability	19
SiO_2@ZnS	water	high index contrast and stability	electrolysis of water	16
PS	water	high surface charge	electrolysis of water	15
PMMA-*co*-PS	water	size and surface charge tunability	electrolysis of water	18
PtBMA	IPG/HC	stability and low cost	low index contrast	current work

[a]Polyferrocenylsilane (PFS) is not a dispersing medium but a polymeric material filling the interstices of SiO_2 opal.

Arsenault et al. developed the technique of so-called photonic ink (P-Ink) in which cross-linked polyferrocenylsilane (PFS) is used to fill the void space of a close-packed silica opal array with an average particle diameter of approximately 200 nm.[8,9] When swollen by a solvent, PFS is an electrochemically active species and thus drives electrical actuation of the space in the opal array along the thickness direction to give rise to color changes. The size of the silica particles was controlled to display the full RGB color range via changes in the volume of PFS. The P-Ink technique was the first example of the use of an opal structure to produce full-color displays, although the cost of the synthesis of PFS is a limiting factor. Other groups demonstrated that an opal-templated porous gel shows faster response in electrical color tuning.[10,11] Following the pioneering research by Ge et al.[12,13] in which magnetically tunable CCA was demonstrated, electrically tunable CCA of charged μ-spheres have been extensively studied because electric field (E-field) is much more versatile than magnetic field as a control signal for a display device.[14−19] Shim et al. reported an electrophoretic full-color display that used emulsion-polymerized polystyrene (PS) μ-spheres dispersed in water.[15] The surface charges on the PS μ-spheres enabled the formation of a stable emulsion owing to electrostatic repulsion, and the particles exhibited a close-packed structure at high solid contents (>10%), which formed an electrically tunable reflective color display. Before the application of an electrical bias, the interparticle spacing corresponded to the Bragg diffraction spacing for red light. Upon the application of a bias, the ordered particles moved to the anode under an electrophoretic driving force, which led to a blue shift in the reflective color. Owing to its highly polar nature, water has been used to disperse charge-stabilized particle systems, such as organic particles[15,18] and ZnS/SiO_2[16] inorganic core−shell particles. However, water possesses critical limitations as a dispersion medium under a voltage bias. First, it easily dissolves metallic impurities, which can be deposited on the cathode surface to produce an unwanted electric current. More seriously, water itself undergoes electrolysis at an overpotential of only ∼1.5 V, which generates heat and H_2 bubbles. To avoid such problems associated with aqueous systems, Lee et al. developed Fe_2O_3/SiO_2 core−shell particles dispersed in propylene carbonate, which formed a quasiamorphous dispersion with a short-range order instead of the long-range order of particles in CCAs.[14] This nonaqueous dispersion of inorganic particles displayed RGB colors as a function of the solid content and was successfully tuned by the application of a voltage owing to the charged particle surfaces. For precise color tuning, particles with reproducible sizes (150−200 nm) and a narrow size distribution are crucial. Metal oxide nanoparticles can be prepared by sol−gel methods.[12,13] For example, the method used for the preparation of sub-micrometer-sized SiO_2 is known as the Stöber process[20] in which an alkoxysilane undergoes base-catalyzed hydrolysis/condensation to produce uniform SiO_2 μ-spheres. However, ensuring reproducibility in particle sizes between different batches in the Stöber synthesis is relatively difficult because fine control of the pH, which plays the key role in determining the particle size, is often hard to achieve. Sol−gel synthesis of TiO_2[17,19] and ZnS[16] μ-spheres in controlled sizes is known to be even more difficult. The emulsion polymerization of organic polymer μ-spheres in an aqueous medium enables much better control of batch-to-batch reproducibility in particle sizes. More importantly, a narrow size distribution can easily be achieved.[21,22] The polymerized μ-spheres are stabilized in water by their surface charges owing to the presence of ionic groups from the initiator. In contrast to water, which has a high dielectric constant ($\varepsilon \sim 80$), hydrocarbons ($\varepsilon < 2$) are not regarded as appropriate media for the charging of particles unless an appropriate surfactant is used in concentrations greater than their critical micelle concentration (CMC).[23,24] There have been comprehensive studies of the charging behavior of polymer particles in nonaqueous liquid media, which was assisted by charged micelles adsorbed onto the surface of the polymer particles.[24−29] Hsu et al. studied the physics associated with the charge stabilization of poly(methyl methacrylate) (PMMA) μ-spheres/sodium di-2-ethylhexyl-sulfosuccinate (AOT)/dodecane from the viewpoints of electrostatics and electrokinetics.[23] They reported the formation of a nonaggregated dispersion by employing AOT as a surfactant. An investigation of the PS μ-sphere/AOT/dodecane system carried out by Cao et al. revealed nonlinear variations in the surface potential of the μ-spheres as a function of the AOT concentration or particle content. These variations were attributed to a dynamic equilibrium between positively and negatively charged AOT micelles, which were preferentially adsorbed onto the surfaces of the μ-spheres to enable charge stabilization of the particle system.[24] AOT has also been used to stabilize the surface-modified Fe_2O_3/SiO_2 inorganic μ-spheres in nonpolar medium in which long-range ordering of μ-spheres showed magnetically tunable structural colors.[13]

In this study, we optimized the charge stabilization of cross-linked poly(*t*-butyl methacrylate) (X-PtBMA) μ-spheres in a paraffinic hydrocarbon (C8−C12) liquid in the presence of AOT. We also investigated the fabrication of a CCA by concentrating a dispersion of the μ-spheres to provide the first demonstration of an electrically tunable all-organic full-color reflective display device. This procedure represents a cost-

DOI: 10.1021/acsami.7b17122
ACS Appl. Mater. Interfaces 2018, 10, 11776−11784

effective and reproducible method for the production of low-power reflective displays.

2. EXPERIMENTAL SECTION

2.1. Preparation of Suspension of Cross-Linked PtBMA μ-Spheres. X-PtBMA μ-spheres were prepared by surfactant-free emulsion polymerization using 2,2′-azobis(2-methylpropionamidine) dihydrochloride (AIBA) as a cationic initiator or potassium persulfate (PPS) as an anionic initiator.[21,22] In a typical synthesis, 20 mL of deionized (DI) water in a round-bottomed reactor was degassed for 30 min under a N_2 atmosphere. At 75 °C, 6 mg of AIBA (or 3 mg of PPS) dissolved in 2 mL of degassed DI water was added to the reactor. A mixture of *t*-butyl methacrylate (tBMA) and ethylene glycol dimethacrylate was rapidly injected, and polymerization proceeded for 1 h. Subsequently, a mixture of 3 mg of AIBA (or 1.5 mg of PPS) and 0.0180 g of tBMA was injected and the reaction was continued for a further 1 h to form a non-crosslinked PtBMA shell on a cross-linked PtBMA core. The emulsions were cooled to room temperature and purified by cycles of repeated centrifugation and redispersion in fresh DI water. As the initial dispersant used for the PtBMA μ-spheres was water, the transfer of the particles to an isoparaffinic liquid was performed as follows. First, X-PtBMA μ-spheres were sedimented by centrifugation at 13 500 rpm for 15 min. After the supernatant was decanted, isopropyl alcohol (IPA) was added and the particles were redispersed by ultrasonication. The amount of IPA added for redispersion was similar to that of the original liquid. After the sedimentation−redispersion cycle in IPA had been repeated three times, a mixture of halocarbon oil (HC; Halocarbon Co., Ltd.) and Isopar G (IPG; ExxonMobil) in a volume ratio of 1:1.7 containing an appropriate amount (1−5 wt %) of AOT was added and final ultrasonication and centrifugation procedures were performed.

2.2. Fabrication of a Reflective Display Device. An electrically tunable display cell was fabricated by infiltrating a colloidal dispersion between two indium tin oxide (ITO) electrodes (2.0 mm × 2.0 mm) sandwiched by a Surlyn (Meltonix 1170-60, Solaronix; thickness = 30 or 60 μm) spacer. Before the cell was assembled, two holes were drilled in the top ITO glass used as the cathode using a 75 mm high-speed minibench drill (KTL SV08010-5001, Dremel TRD346, C.R. Laurence), and the ITO glass was rinsed with ethanol. After the CCA dispersion was infiltrated into a channel space, both holes were sealed with UV-curable resin (Secure CP-7426, Fotopolymer), which was cured using a 100 W UV lamp (Execure 4000-D, Hoya Candeo Optronics).

2.3. Characterizations. The sizes and zeta potentials (ζ) of the X-PtBMA μ-spheres were measured by a scanning electron microscope (S-4700, Hitachi) and a ζ analyzer (ELSZ-1000, Otsuka Electronics), respectively. The viscosity of IPG/HC mixture was measured by a viscometer (DVII + Pro, Brookfield).

2.4. Electrical Tuning of the Display Device. The voltage biases applied to the display cells were controlled using a potentiostat (CompactStat, Ivium), and the reflectance spectra of the display cells were recorded using a fiber-optic UV−vis spectrometer (AvaSpec, Avantes) coupled to a reflected light microscope (Zeiss Axioplan EL-Einsatz, Carl Zeiss) equipped with an objective lens (20×/0.30 NA). The changes in color response as a result of E-tuning were monitored using a digital camera (DSLR-A550; Sony).

3. RESULTS AND DISCUSSION

3.1. Preparation of CCA Based on X-PtBMA μ-Spheres in an Organic Medium Assisted by AOT. To avoid the problem of the electrolysis of water upon the application of a voltage bias,[30] nonpolar organic liquids were investigated for the production of a polymeric CCA. A mixture of halocarbon oil (HC; Halocarbon Co., Ltd.,) and Isopar G (IPG; ExxonMobil) was adopted because it has been effectively used for dispersing charge-stabilized nanoparticles in E ink technology. The weight ratio between HC and IPG was optimized at 1:1.7 to achieve a mass density of 1 g cm^{-3}, which is slightly lower than that of X-PtBMA μ-spheres (~1.02 g cm^{-3}) prepared by emulsion polymerization. X-PtBMA was rationally chosen as a polymeric μ-sphere system because it is highly dispersible in HC/IPG. In addition, the synthesis of the size-controlled X-PtBMA is simple and cost-effective.[21,22] Other μ-spheres based on polymers such as PS or PMMA, which were formed by emulsion polymerization, were also investigated, but these readily aggregated in this medium. Hence, highly uniform X-PtBMA particles with different mean diameters of 170 and 200 nm were synthesized using both cationic and anionic radical initiators, which were denoted as CAT-X-PtBMA170, AN-X-PtBMA170, CAT-X-PtBMA200, and AN-X-PtBMA200, respectively. Scanning electron microscopy images of four different X-PtBMA μ-spheres are shown in Figure 1. Although

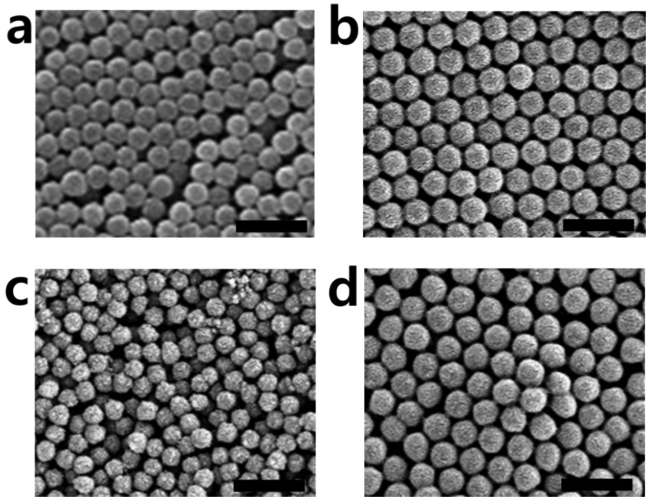

Figure 1. Scanning electron microscopy images of X-PtBMA μ-spheres used in this study: (a) CAT-X-PtBMA170, (b) CAT-X-PtBMA200, (c) AN-X-PtBMA170, and (d) AN-X-PtBMA200. In (a) and (b), the formation of the X-PtBMA particles was initiated by the cationic initiator AIBA, whereas in (c) and (d), the formation of the X-PtBMA particles was initiated by the anionic initiator PPS. The scale bar in each image corresponds to 500 nm.

non-crosslinked PtBMA partially dissolved in HC/IPG that contained AOT, the cross-linking of PtBMA μ-spheres enabled the formation of a uniform dispersion in this medium, as well as the prerequisites of an appropriate particle size and size distribution for the formation of a CCA, the colloidal system, also has to be completely dispersible without aggregation in a given solvent to form a stable CCA that can display a clear reflective color. This can be accomplished by the charge stabilization of particles on the basis of the classical theory of Derjaguin, Landau, Verwey, and Overbeek.[31,32]

In a hydrocarbon-based liquid, polymeric μ-spheres can bear suitable surface charges with the assistance of charged micelles of surfactant molecules.[23] AOT, which is a surfactant composed of one anionic sulfosuccinate head group and two branched alkyl tail groups, forms inverse micelles in nonpolar hydrocarbon solvents, as shown schematically in Figure 2. The role of inverse micelles of AOT in a nonpolar medium is to provide sufficient charge density on the surface of X-PtBMA particles, which otherwise bear negligible amounts of charge and easily aggregate. The mechanism of the charging of μ-spheres in nonpolar media containing AOT is, however, still not clearly understood owing to the complex formation of anionic and cationic micelles and their adsorption behaviors.[26] Each

DOI: 10.1021/acsami.7b17122
ACS Appl. Mater. Interfaces 2018, 10, 11776−11784

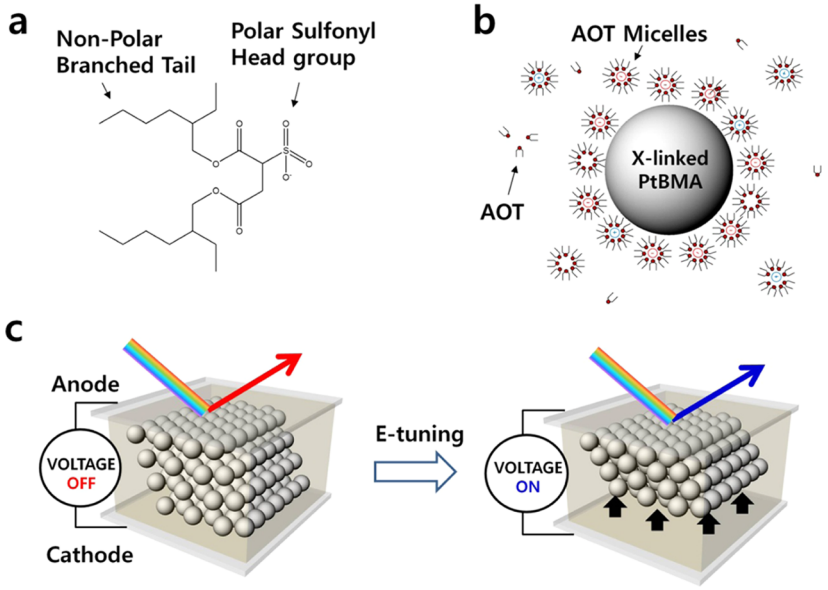

Figure 2. (a) Molecular structure of AOT. (b) Schematic showing the adsorption of charged micelles of AOT in HC/IPG onto the surface of an X-PtBMA μ-sphere above the CMC of AOT. Negatively charged micelles are preferentially adsorbed to provide a negative surface potential on the μ-sphere. (c) Schematic of the all-organic electrically tunable reflective display. Charge stabilization of μ-spheres enables the formation of a polymeric CCA at high contents (>30 wt %) of μ-spheres in the HC/IPG medium, which displays a structural color due to the Bragg diffraction of incident light. Electrophoretic migration of μ-spheres upon the application of a voltage alters the interparticle spacing and thus changes the structural color.

aqueous dispersion of X-PtBMA was transferred to isopropyl alcohol (IPA), which served as an intermediate medium, and was finally dispersed in HC/IPG premixed with AOT. The AOT content in HC/IPG was controlled in the range from 0.5 to 10 wt %, which largely exceeds the CMC of AOT in this liquid.[26] It was found that X-PtBMA μ-spheres surrounded by AOT formed stable dispersions in HC/IPG at relatively high AOT concentrations (>1 wt %). More importantly, all four μ-sphere systems formed a CCA that displayed the respective structural colors when the weight percentage of μ-spheres in each dispersion reached ~30 wt %. The CCAs formed from CAT-X-PtBMA170 and AN-X-PtBMA170 exhibited green reflective colors within the HC/IPG/AOT dispersant (Figure S1, Supporting Information), whereas those formed from particles with sizes of 200 nm displayed red colors.

To investigate the charge stabilization of X-PtBMA μ-spheres in HC/IPG, the ζ of AN-X-PtBMA200 and CAT-X-PtBMA200 were measured at various AOT concentrations. The μ-sphere content was fixed at 10^{-3} wt % for the measurements of the ζ values. As shown in Figure 3, the surface potential exhibited nonlinear behavior as a function of the AOT content, which was in accordance with the results reported by a previous investigation indicating a preferential sorption of anionic micelles followed by subsequent saturation and adsorption of cationic micelles with increasing AOT concentration.[24] However, it should be noted that our dispersions were prepared over a much higher range of AOT concentrations (up to 10%) compared to that of dispersions in the previous study.[24] Typically, CAT-X-PtBMA μ-spheres exhibited positive ζ values at low AOT contents, which can be attributed to the protonated amidine group (see the Experimental Section) of the cationic initiator. The absolute values of ζ decreased with an increase in the AOT content, which was probably due to charge compensation upon the preferential adsorption of anionic micelles. AN-X-PtBMA200 exhibited an opposite (increasing) tendency in the absolute values of ζ at AOT

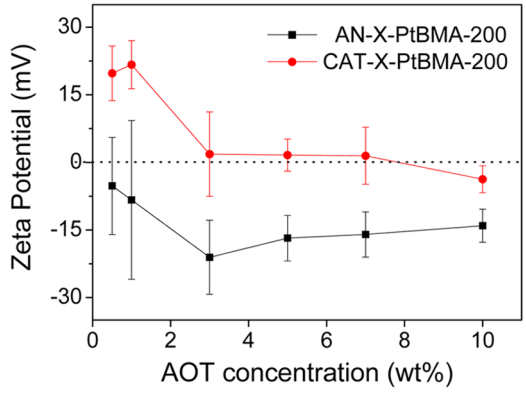

Figure 3. ζ values of AN-X-PtBMA200 and CAT-X-PtBMA200 measured at 25 °C in HC/IPG at various AOT concentrations. The particle concentration was set to 10^{-3} wt %. The absolute values of ζ decreased for CAT-X-PtBMA200 with an increase in the AOT concentration, whereas those of AN-X-PtBMA200 increased with an increase in the AOT concentration up to 3 wt %. At AOT concentrations higher than 3 wt %, the ζ values of AN-X-PtBMA200 decreased.

contents of up to 3–4 wt %, which can be explained in an analogous manner to the behavior of cationic μ-spheres by the adsorption of anionic micelles. For both μ-sphere systems, saturation of the ζ values was observed at AOT contents of greater than ~5 wt %, which can be explained by the complete occupation of the particle surfaces by anionic AOT micelles, followed by the additional adsorption of positively charged micelles to compensate the surface potential, as can be seen for AN-X-PtBMA200.[26] Nonetheless, the tendency observed in the ζ values of the PtBMA μ-spheres/HC/IPG/AOT system, as shown in Figure 3, may not directly apply to the highly concentrated dispersions of particles (>30 wt %) that were actually employed for the fabrication of CCA displays in this study.

DOI: 10.1021/acsami.7b17122
ACS Appl. Mater. Interfaces 2018, 10, 11776–11784

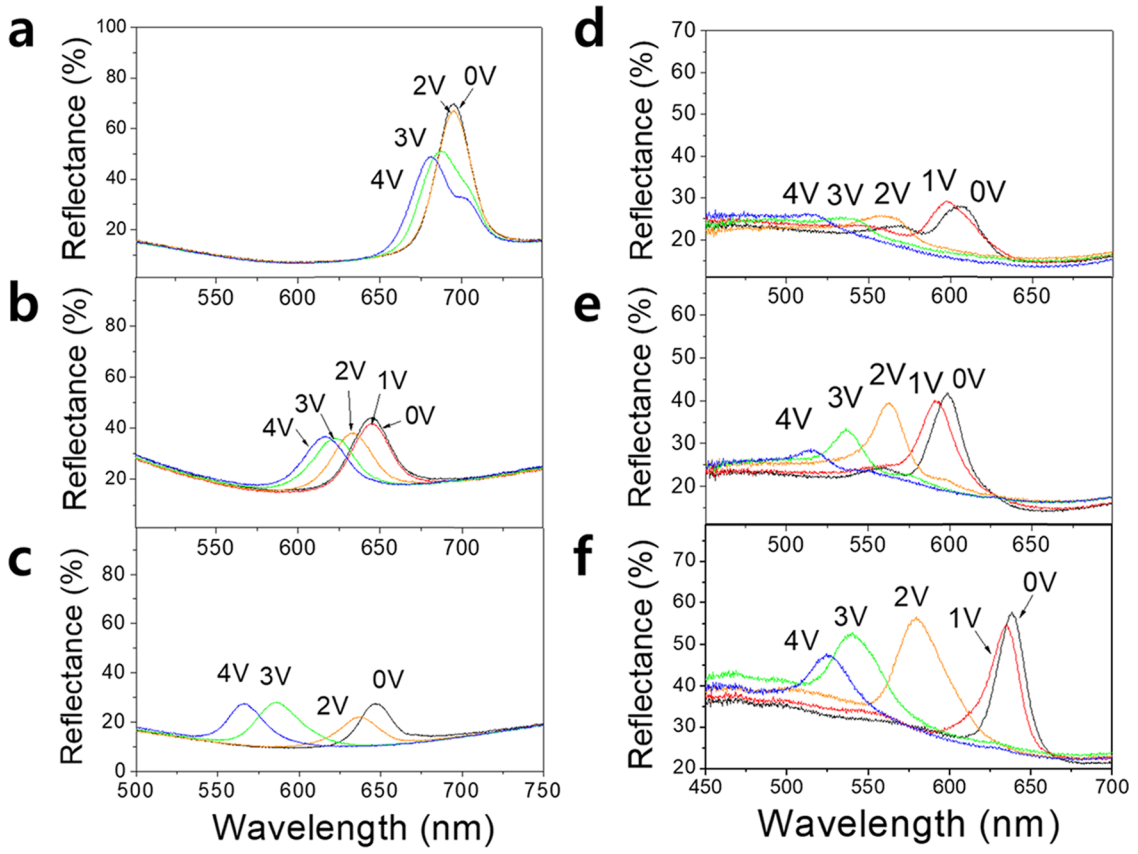

Figure 4. E-tuning of peak reflectance observed for the CCAs prepared from CAT-X-PtBMA200 (a–c) and AN-X-PtBMA200 (d–f) in HC/IPG at varying AOT concentrations. The respective concentrations of AOT were 1 wt % (a, d), 3 wt % (b, e), and 5 wt % (c, f), and the μ-sphere contents were ~30% for all six CCAs. Over the voltage bias range from 0 to 4 V, an increase in the AOT concentration resulted in an improvement in the E-tunability of both systems. The general blue shift in the peaks and the decrease in the peak height with an increase in the AOT concentration for CAT-X-PtBMA200 showed opposite tendencies to those for AN-X-PtBMA200, for which a red shift in the peaks recorded at zero bias and an increase in the peak height with an increase in the AOT concentration were observed. These tendencies of the two oppositely charged colloidal systems are in accordance with the variations in the ζ values with respect to the AOT concentration.

3.2. Electrical Color Tuning of the X-PtBMA CCA Reflective Display. In the presence of an electric field (E-field) applied between two indium tin oxide (ITO) electrodes, reflectance spectra were recorded for CCAs at three different AOT contents, as shown in Figure 4. Within the HC/IPG medium at AOT contents of greater than 1 wt %, the CCAs formed from both CAT-X-PtBMA200 and AN-X-PtBMA200 exhibited blue shifts in the reflection peaks under a voltage bias. A blue shift in the reflective color displayed by a CCA within an E-field implies that the colloidal particles migrated electrophoretically toward an electrode and the interparticle distances decreased along the direction of the E-field. Figure 4a reveals that the CCA formed from CAT-X-PtBMA200 with 1 wt % AOT displayed a highly reflective color and a long diffraction wavelength owing to the charged particles and the well-aligned CCA, as can be expected from the ζ values of CAT-X-PtBMA200 shown in Figure 3. However, electrical tuning (E-tuning) of the CCA formed from CAT-X-PtBMA200 with 1% AOT led to only slight changes in the peak wavelengths, as shown in Figure 4a. An increase in the AOT content in CAT-X-PtBMA200 apparently brought about a blue shift in the reflection peak displayed by the CCA in the absence of a voltage bias. In addition, the reflective colors became less intense with an increase in the AOT content, as shown in Figure 4b,c. The blue shift and reduction in the intensity of the reflective colors with an increase in the AOT content can be attributed to the reduction in ζ values caused by charge compensation on the surfaces of the cationic μ-spheres. The charge density on the surface of a μ-sphere is directly related to the separation between μ-spheres and the crystallinity of the CCA. A reduction in the value of ζ implies a decrease in the thickness of the electrical double layer (EDL), a decrease in interparticle distances, and a reduction in the crystallinity of the CCA.

On the other hand, Figure 4b,c also shows improvements in the E-tunability of the color responses with an increase in the AOT content, which seems to be inconsistent with the tendency of the electrophoretic mobility (μ_e) upon reduction of ζ, as shown by eq (1)[33]

$$\mu_e = 2\varepsilon_r\varepsilon_0\zeta/3\eta \quad (1)$$

where ε_r, ε_0, and η denote the dielectric constants of the medium, free space, and the solvent viscosity, respectively. It should be noted that the ζ values of the concentrated CCA might be different from those shown in Figure 3, which represent a situation in which the particles were substantially diluted (10^{-3} wt %). In addition, the Hückel theory predicts that the μ_e value of a charged particle depends not only on the value of ζ but also on that of the dielectric constant (ε_r) of a given solvent in conditions in which the EDL is thick.[33] At a high AOT content, the competing contributions of an increase in the value of ε_r and a decrease in that of ζ might have affected

DOI: 10.1021/acsami.7b17122
ACS Appl. Mater. Interfaces 2018, 10, 11776–11784

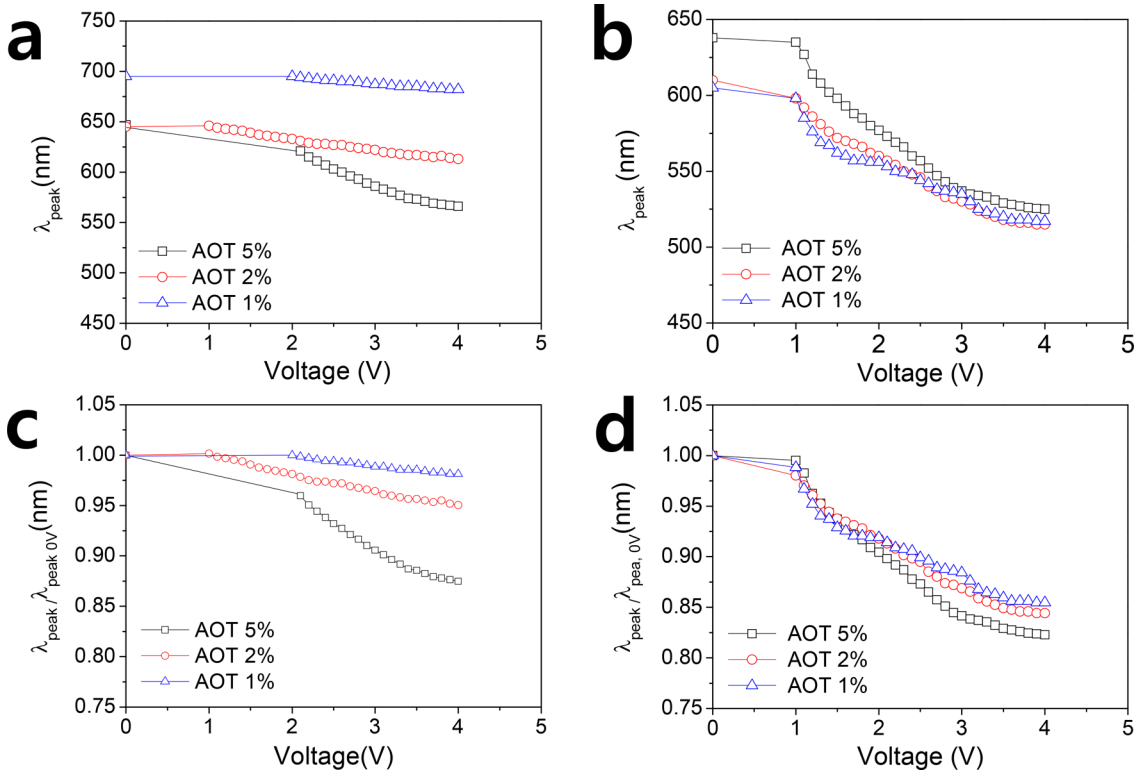

Figure 5. Plots of λ_{peak} (a, b) and $\lambda_{peak}/\lambda_{peak,0V}$ (c, d) obtained from the full reflectance spectra of the CCAs prepared from CAT-X-PtBMA200 (a, c) and AN-X-PtBMA200 (b, d) over the voltage bias range from 0 to 4 V. In comparison with the CCAs formed from CAT-X-PtBMA200, those formed from AN-X-PtBMA200 evidently displayed higher color tunability ($d\lambda_{peak}/dV$) over the entire voltage range, irrespective of the AOT concentration.

the μ_e value of the cationic μ-spheres to bring about an improvement in E-tunability, as demonstrated in Figure 4c. On the other hand, we observed that the colloidal dispersion of CAT-X-PtBMA200 at high AOT concentrations was readily gelled during the preparation of the CCA and therefore the preparation of the CCA and the subsequent E-tuning were poorly reproducible. When AN-X-PtBMA200 was employed for the preparation of the CCA, an increase in the E-tunability of the color response was achieved with much higher reproducibility in comparison to that observed for CAT-X-PtBMA200. As shown in Figure 4d–f, increases in the AOT content from 1 to 5% led to slight increases in the difference in the reflection peak wavelength ($\Delta\lambda_{peak}$) over the voltage bias range from 0 to 4 V. The peak recorded in the absence of an E-field underwent a red shift with an increase in the AOT content, as was expected from the variation in the ζ values shown in Figure 3. It is noteworthy that an increase in the AOT content in the dispersion of AN-X-PtBMA200 increased the intensity of the reflective color, as demonstrated by the increase in the reflection peak heights in Figure 4d–f, which displays a tendency opposite to those for the CCAs formed from CAT-X-PtBMA200. From these tendencies of CCAs formed from AN-X-PtBMA200, which exhibit brighter reflective colors with an increase in the AOT concentration, it can be confirmed that an increase in the ζ value on a μ-sphere results in the formation of a higher-quality CCA. CCAs with higher AOT concentrations (>7 wt %) were also investigated, but no distinguishable improvement could be observed. In Figure 5, the values of the reflection peak wavelength (λ_{peak}), together with these values normalized to the value of λ_{peak} at 0 V ($\lambda_{peak,0V}$), are plotted against the applied voltage bias to facilitate the understanding of the characteristic responses to E-tuning of the CCAs investigated in this study. As shown in Figure 5c,d, for the CCAs formed from CAT-X-PtBMA, the E-tunability ($d\lambda_{peak}/dV$) was highly dependent upon the AOT concentration, whereas better E-tunability was evidently displayed by those formed from AN-X-PtBMA, regardless of the AOT content. Although a direct correlation between the plot of ζ versus the AOT content shown in Figure 3 and the plots of λ_{peak} for different AOT contents shown in Figure 5 would be inappropriate because of the great difference between the concentration ranges of μ-spheres, it was clearly found that the CCAs formed from the AN-X-PtBMA series with an AOT content as high as 5 wt % constituted highly reflective and highly E-tunable colloidal display systems.

Using the CCA formed from AN-X-PtBMA in HC/IPG containing 5 wt % AOT as an optimized example of an all-organic display, its E-tunable color response was rigorously investigated. Figure 6 shows the changes in the reflective colors and reflection spectra displayed by a single all-organic CCA cell with an area of 1 × 1 cm^2 and a thickness of 20 μm with variations in the voltage bias.

Starting from a red color in the absence of an E-field, the color changes were monitored while increasing the voltage bias. At a voltage bias greater than 3 V, the E-tunability was significantly decreased, as shown in Figure 4d. More importantly, the reflection peak started to decrease in intensity. At a bias of 10 V, substantial peak broadening also occurred and the corresponding reflective color appeared as pale blue. Using a thicker display cell, the colors at high voltages could be improved because the diffraction of light from the CCA was strengthened (Figure S2, Supporting Information). Weakening

DOI: 10.1021/acsami.7b17122
ACS Appl. Mater. Interfaces 2018, 10, 11776–11784

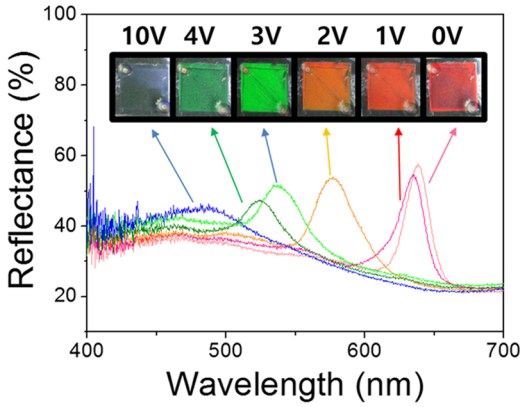

Figure 6. Changes in the reflective colors (inset) and reflection spectra displayed by a single all-organic CCA cell (area = 1 × 1 cm^2 and thickness = 25 μm) with variations in the voltage bias. The single cell was filled with a CCA dispersion of 40% AN-X-PtBMA200 in HC/IPG containing 5 wt % AOT.

and broadening of the reflection peak imply that the long-range ordering of the colloidal array is partially disrupted. It has been suggested that a long-range ordering requires high surface charge; thus, our system which has relatively low ζ is thought to in part have short-range ordered assembly.[30] More about the particle ordering issue will be discussed in the later section.

3.3. Characteristic Features of the Reflective Display of CCA Formed from X-PtBMA. One of the most intriguing features of the all-organic display developed in this study is its very low operating current in comparison with that in water. As shown in Figure 7a, the operating current was measured in a typical display cell consisting of two ITO electrodes (area of 1 × 1 cm^2 and thickness of 25 μm) filled with AN-X-PtBMA200 in HC/IPG/AOT when programmed voltage biases of 2, 3, and 4 V were applied. The voltage program was chosen because voltages of 2, 3, and 4 V, respectively, generated typical RGB colors in this CCA system. The maximum electric current, which was recorded at a voltage bias of 4 V, was measured to be ~1.5 × 10^{-6} A, which is an extremely low value (6 μW cm^{-2}) when the large cell area (1 cm^2) is taken into consideration. In general, the display device with a power density lower than 10 mW cm^{-2} is considered to have an ultralow power consumption level.[1] Although the power consumption for additional circuit control is not taken into account, the ultralow power density to operate our all-organic CCA is worthwhile to note. In the HC/IPG medium, the solubilities of metal ions are very low in comparison with those in a polar medium such as water, and thus the generation of an unwanted electric current by redox reactions is minimized.

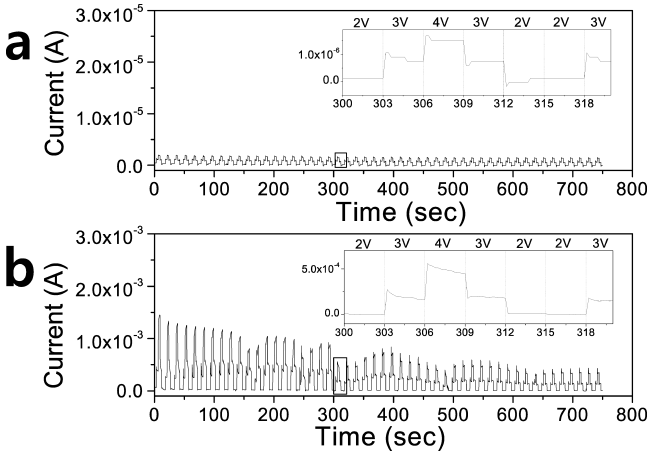

Figure 7. Operating current measured for reflective display cells containing CCAs formed from AN-X-PtBMA200 μ-spheres dispersed in (a) HC/IPG/5% AOT and (b) DI water. Preprogrammed voltage biases of 2, 3, and 4 V, as indicated in the insets, were applied to both cells.

For comparison, a CCA formed from the same AN-X-PtBMA200 μ-spheres dispersed in deionized (DI) water was prepared and a display cell with the same thickness and area was fabricated. Upon application of the same sequence of voltage biases, the current initially measured at a bias of 4 V was ~1.5 × 10^{-3} A, which was 1000 times higher than that measured in the all-organic display cell. Ultralow operating current in an electrical device implies two major advantages, namely, low power consumption and a long device lifetime. The current in the all-organic display was found to be stable over repeated voltage bias cycles during an operating period of several hours, whereas the CCA dispersed in water exhibited a significant decrease in current, together with fluctuations in its values, which were presumably due to the significant redox reactions at the electrodes that can take place within the given range of voltage biases. To confirm whether redox reactions had occurred on the electrode surfaces, the color of ITO glass electrodes in an aqueous cell after an operating period of 1 h was compared with that of electrodes in an all-organic cell. Significant darkening of the cathode surface was observed in the aqueous cell, which implied that the deposition of metallic impurities had occurred owing to the low overpotentials in the aqueous medium (Figure S3, Supporting Information).

The rate of change in the color displayed by the all-organic display was measured during an instantaneous voltage bias of 3 V, which induces a red-to-green color change. Measurements of time-dependent reflectance were carried out on an AN-X-PtBMA200 display cell with a thickness of 25 μm. In Figure 8, time-dependent changes in the value of λ_{peak} upon the application of a voltage bias are plotted. At 2 s, a direct current (DC) bias of 3 V was applied to induce a subsequent exponential decay in the value of λ_{peak}, accompanied by a blue

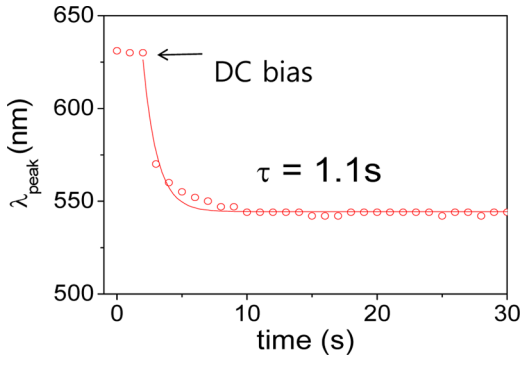

Figure 8. Plot of time-dependent changes in the peak reflectance of an all-organic display cell upon the application of an instantaneous voltage bias of 3 V at 2 s. A display cell with a thickness of 25 μm comprising AN-X-PtBMA200 in HC/IPG containing 5 wt % AOT was used. Upon the application of a DC voltage bias, the value of λ_{peak} was observed to decrease exponentially from 627 to 540 nm. The data were fitted to an exponential decay function with a decay time constant of 1.1 s.

DOI: 10.1021/acsami.7b17122
ACS Appl. Mater. Interfaces 2018, 10, 11776−11784

shift in the reflective color. The data after 2 s were fitted to a first-order exponential decay function to give a time constant (τ) of 1.1 s.

The time required for the color change was longer than that for the CCA formed from AN-X-PtBMA200 in water (τ_{water} = 0.5 s) owing to the lower dielectric constant, as well as the higher viscosity (1.3 cP), of HC/IPG, both of which affect the mobility of μ-spheres. A graph of λ_{peak} versus time for the aqueous CCA is shown in the Supporting Information (Figure S4). In addition to the demonstration in Figure 7 where a low operating current is maintained with voltage biases, the reversibility of reflective color under repeated voltage bias was also examined, from which a stable voltage-driven color changing was confirmed (Figure S5, Supporting Information).

In both the presence and absence of an E-field, the angular dependences of the reflective colors were examined for AN-X-PtBMA200 in HC/IPG/AOT. With normal incidence of white light, angle-dependent reflection of colors was observed in the range from 0 to 50°. The apparent colors of a reflective display showing typical RGB colors at voltage biases of 0, 3, and 6 V were almost unchanged regardless of the viewing angle (Figure S6, Supporting Information). However, a slight decrease in the value of λ_{peak} (~1.1%) was measured for red reflected light at a bias of 0 V and a viewing angle of 50° (Figure 9). The angular

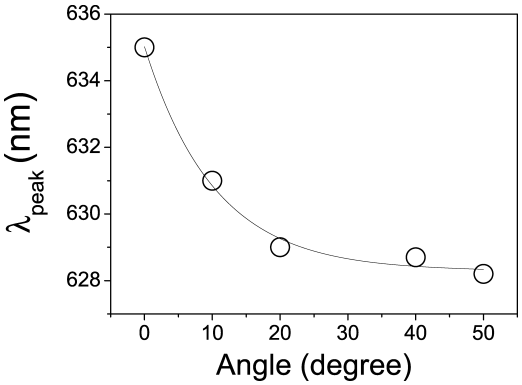

Figure 9. Angular dependence of the diffraction wavelength measured for a CCA formed from AN-X-PtBMA200 in HC/IPG containing 5 wt % AOT in absence of voltage bias.

dependence of the diffraction wavelength, as shown in Figure 9, is, however, not as great as that predicted by the modified Bragg law for a face-centered cubic opal structure, which is given by the equation $1.633 \cdot n_{eff} \cdot d \sin\theta = \lambda$, where n_{eff} is the effective refractive index and d is the distance between particles in a highly ordered opal lattice. A similar low angular dependence of the optical response was reported in recent studies in which a quasiamorphous colloidal structure was proposed rather than the formation of a highly ordered CCA.[14] In a quasiamorphous colloidal array, short-range ordered colloidal arrays at high concentration develop the reflective color and the bandwidth of the reflectance peak appears to be generally broader than that of CCA.[14,34] A slight angular dependence of reflective colors observed in our system implies that the structure of colloidal arrays should be a moderately ordered CCA in which a quasiamorphous character coexists. In any event, a relatively low angular dependence of the structural colors, together with the advantageous features of a low operating current and the ability to generate RGB colors in a single pixel, hold the potential for the development of highly efficient reflective displays upon further engineering of the current device.

4. CONCLUSIONS

In summary, we have successfully demonstrated electrically tunable all-organic full-color displays using CCAs formed from charged cross-linked PtBMA μ-spheres in an HC/IPG liquid medium in the presence of inverse micelles of AOT. Four μ-spheres with different particle sizes were prepared using different initiators for testing as E-tunable CCAs. At a high solid content (>30 wt %) and a high concentration of AOT (>1 wt %), cross-linked PtBMA μ-spheres with a diameter of 200 nm formed a highly stable CCA, which exhibited changes in structural color on the application of a voltage bias. E-tuning of the RGB structural colors in an all-organic display cell with an area of 1 cm^2 was revealed to consume an extremely low operating current (1.5×10^{-6} A at a bias of 4 V), which was lower than that of a CCA in a water dispersant by a factor of 1000.

■ ASSOCIATED CONTENT

Supporting Information

The Supporting Information is available free of charge on the ACS Publications website at DOI: 10.1021/acsami.7b17122.

Photographs showing the CCA dispersions of X-PtBMA in HC/IPG containing 2 wt % AOT (Figure S1); photographs showing the reflective colors of AN-X-PtBMA200/IPG/HC/5% AOT in display cells with different thicknesses (25 vs 60 μm) (Figure S2); photographs showing the bottom ITO glasses used for E-tuning an aqueous CCA and an all-organic CCA after 750 voltage bias cycles were applied to both cells (Figure S3); time-dependent changes in the value of λ_{peak} upon the application of a bias of 0−3 V to an aqueous CCA display prepared from 20 wt % AN-X-PtBMA200 in DI water (Figure S4); changes in reflection peak position and operating current under the repeated voltage biases between 0 and 3 V (Figure S5); angle-dependent reflectance spectra and photographs of a display from the CCA formed from AN-X-PtBMA200/IPG/HC/5% AOT (Figure S6) (PDF)

■ AUTHOR INFORMATION

Corresponding Author

*E-mail: wonmoklee@sejong.ac.kr.

ORCID

Wonmok Lee: 0000-0001-6757-885X

Author Contributions

§K.H.K. and E.P. contributed equally.

Notes

The authors declare no competing financial interest.

■ ACKNOWLEDGMENTS

This study was financially supported by the Basic Science Research Program through the National Research Foundation of Korea (NRF), which is funded by the Ministry of Science, ICT and Future Planning (Grant No. 2016R1A2B4012313), and partially supported by the Technology Innovation Program (Grant No. 10062366) funded by the Ministry of Trade, Industry & Energy, Korea.

DOI: 10.1021/acsami.7b17122
ACS Appl. Mater. Interfaces 2018, 10, 11776−11784

REFERENCES

(1) Fernández, M. R.; Casanova, E. Z.; Alonso, I. G. Review of Display Technologies Focusing on Power Consumption. *Sustainability* **2015**, *7*, 10854−10875.

(2) Dunmur, D.; Sluckin, T. *Soap, Science, and Flat-Screen TVs: A History of Liquid Crystals*; Oxford University Press: Oxford, 2011.

(3) Jacobson, J.; Comiskey, B. Nonemissive Displays and Piezoelectric Power Supplies Therefor. 5930026, 1996.

(4) Einkgroup.com. E Ink Holdings—About Us. www.einkgroup.com.

(5) Bellingeri, M.; Chiasera, A.; Kriegel, I.; Scotognella, F. Optical properties of periodic, quasi-periodic, and disordered one dimensional photonic structures. *Opt. Mater.* **2017**, *72*, 403−421.

(6) Nucara, L.; Greco, F.; Mattoli, V. Electrically responsive photonic crystals: a review. *J. Mater. Chem. C* **2015**, *3*, 8449−8467.

(7) Lu, Y.; Meng, C.; Xia, H.; Zhang, G.; Wu, C. Fast electrically driven photonic crystal based on charged block copolymer. *J. Mater. Chem. C* **2013**, *1*, 6107−6111.

(8) Arsenault, A. C.; Puzzo, D. P.; Manner, I.; Ozin, G. A. Photonic-crystal full-colour displays. *Nat. Photonics* **2007**, *1*, 468−472.

(9) Puzzo, D. P.; Arsenault, A. C.; Manner, I.; Ozin, G. A. Electroactive Inverse Opal: A Single Material for All Colors. *Angew. Chem., Int. Ed.* **2009**, *48*, 943−947.

(10) Jiang, Y.; Xu, D.; Li, X.; Lin, C.; Li, W.; An, Q.; Tao, C.; Tang, H.; Li, G. Electrothermally driven structural colour based on liquid crystal elastomers. *J. Mater. Chem.* **2012**, *22*, 11943−11949.

(11) Ueno, K.; Matsubar, K.; Watanabe, M.; Takeoka, Y. An Electro- and Thermochromic Hydrogel as a Full-Color Indicator. *Adv. Mater.* **2007**, *19*, 2807−2812.

(12) Ge, J.; Hu, Y.; Yin, Y. Highly Tunable Superparamagnetic Colloidal Photonic Crystals. *Angew. Chem.* **2007**, *119*, 7572−7575.

(13) Ge, J.; He, L.; Goebl, J.; Yin, Y. Assembly of Magnetically Tunable Photonic Crystals in Nonpolar Solvents. *J. Am. Chem. Soc.* **2009**, *131*, 3484−3486.

(14) Lee, I.; Kim, D.; Kal, J.; Baek, H.; Kwak, D.; Go, D.; Kim, E.; Kang, C.; Chung, J.; Jang, Y.; Ji, S.; Joo, J.; Kang, Y. Quasi-Amorphous Colloidal Structures for Electrically Tunable Full-Color Photonic Pixels with Angle-Independency. *Adv. Mater.* **2010**, *22*, 4973−4977.

(15) Shim, T. S.; Kim, S.-H.; Sim, J. Y.; Lim, J.-M.; Yang, S.-M. Dynamic Modulation of Photonic Bandgaps in Crystalline Colloidal Arrays Under Electric Field. *Adv. Mater.* **2010**, *22*, 4494−4498.

(16) Han, M. G.; Shin, C. G.; Jeon, S.-J.; Shim, H. S.; Heo, C.-J.; Jin, H.; Kim, J. W.; Lee, S. Y. Full Color Tunable Photonic Crystal from Crystalline Colloidal Arrays with an Engineered Photonic Stop-Band. *Adv. Mater.* **2012**, *24*, 6438−6444.

(17) Shim, H. S.; Lim, J.; Shin, C. G.; Jeon, S.-J.; Han, M. G.; Lee, J.-K. Spectral reflectance switching of colloidal photonic crystal structure composed of positively charged TiO_2 nanoparticles. *Appl. Phys. Lett.* **2012**, *100*, No. 063113.

(18) Han, M. G.; Heo, C.-J.; Shin, C. G.; Shim, H. S.; Kim, J. W.; Jin, Y. W.; Lee, S. Y. Electrically tunable photonic crystals from long-range ordered crystalline arrays composed of copolymer colloids. *J. Mater. Chem. C* **2013**, *1*, 5791−5798.

(19) Luo, Y.; Zhang, J.; Sun, A.; Chu, C.; Zhou, S.; Guo, J.; Chen, T.; Xu, G. Electric field induced structural color changes of SiO_2@TiO_2 core−shell colloidal suspensions. *J. Mater. Chem. C* **2014**, *2*, 1990−1994.

(20) Stöber, W.; Fink, A.; Bohn, E. Controlled growth of monodisperse silica spheres in the micron size range. *J. Colloid Interface Sci.* **1968**, *26*, 62−69.

(21) Tanrisevert, T.; Okay, O.; Sönmezoğlu, I. Ç. Kinetics of Emulsifier-Free Emulsion Polymerization of Methyl Methacrylate. *J. Appl. Polym. Sci.* **1996**, *61*, 485−492.

(22) Kim, S.-G.; Seo, Y.-G.; Cho, Y.-J.; Shin, J.-S.; Gil, S.-C.; Lee, W.-M. Optimization of Emulsion Polymerization for Submicron-Sized Polymer Colloids towards Tunable Synthetic Opals. *Bull. Korean Chem. Soc.* **2010**, *31*, 1891−1896.

(23) Hsu, M. F.; Dufresne, E. R.; Weitz, D. A. Charge Stabilization in Nonpolar Solvents. *Langmuir* **2005**, *21*, 4881−4887.

(24) Cao, H.; Cheng, Y.; Huang, P.; Qi, M. Investigation of charging behavior of PS particles in nonpolar solvents. *Nanotechnology* **2011**, *22*, No. 445709.

(25) Strubbe, F.; Verschueren, A. R. M.; Schlangen, L. J. M.; Beunis, F.; Neyts, K. Generation current of charged micelles in nonaqueous liquids: Measurements and simulations. *J. Colloid Interface Sci.* **2006**, *300*, 396−403.

(26) Smith, P. G.; Patel, M. N.; Kim, J.; Milner, T. E.; Johnston, K. P. Effect of Surface Hydrophilicity on Charging Mechanism of Colloids in Low-Permittivity Solvents. *J. Phys. Chem. C* **2007**, *111*, 840−848.

(27) Sainis, S. K.; Germain, V.; Mejean, C. O.; Dufresne, E. R. Electrostatic Interactions of Colloidal Particles in Nonpolar Solvents: Role of Surface Chemistry and Charge Control Agents. *Langmuir* **2008**, *24*, 1160−1164.

(28) Wang, X.; Xu, S.; Liang, C.; Li, H.; Sun, F.; Xu, W. Enriching PMMA nanospheres with adjustable charges as novel templates for multicolored dye@PMMA nanocomposites. *Nanotechnology* **2011**, *22*, No. 275608.

(29) Guo, Q.; Lee, J.; Singh, V.; Beherns, S. H. Surfactant mediated charging of polymer particles in a nonpolar liquid. *J. Colloid Interface Sci.* **2013**, *392*, 83−89.

(30) Shim, H. S.; Shin, C. G.; Heo, C.-J.; Jeon, S.-J.; Jin, H.; Kim, J. W.; Jin, Y. W.; Lee, S. Y.; Lim, J.; Han, M. G.; Lee, J.-K. Stability enhancement of an electrically tunable colloidal photonic crystal using modified electrodes with a large electrochemical potential window. *Appl. Phys. Lett.* **2014**, *104*, No. 051104.

(31) Derjaguin, B.; Landau, L. Theory of the stability of strongly charged lyophobic sols and of the adhesion of strongly charged particles in solution of electrolytes. *Prog. Surf. Sci.* **1993**, *43*, 30−59.

(32) Verwey, E. J. W.; Overbeek, J. T. G. *Theory of the Stability of Lyophobic Colloids: The Interactions of Sol Particles Having an Electric Double Layer*; Elsevier, 1948.

(33) O'Brien, R. W.; White, L. R. Electrophoretic mobility of a spherical colloidal particle. *J. Chem. Soc., Faraday Trans. 2* **1978**, *2*, 1607−1626.

(34) Takeoka, Y. Angle-independent Structural Coloured Amorphous Arrays. *J. Mater. Chem.* **2012**, *22*, 23299−23309.

DOI: 10.1021/acsami.7b17122
ACS Appl. Mater. Interfaces 2018, 10, 11776−11784